Journal of Building Engineering 120 (2026) 115441

Contents lists available at ScienceDirect

Journal of Building Engineering

journal homepage: www.elsevier.com/locate/jobe

An extended cellular automaton model for crowd evacuation under multi-storey building with ControlNet

Tong Lu [a,b], Rong Deng [a,b], Yuxin Zhang [a,*], Saizhe Ding [a,b], Xinyan Huang [a,b,**]

[a] Research Center for Smart Urban Resilience and Firefighting, Department of Building Environment and Energy Engineering, The Hong Kong Polytechnic University, Hong Kong
[b] Research Institute for Sustainable Urban Development, The Hong Kong Polytechnic University, Hong Kong

ARTICLE INFO

Keywords:
Pedestrian evacuation
Cellular automaton
Numerical simulation
ControlNet
Fire Safety
High-rise building

ABSTRACT

Vertical evacuation safety in high-rise buildings presents a key challenge for urban resilience. This study proposes an automated evacuation modelling method for high-rise buildings that combines deep learning and an extended cellular automaton model, which can achieve rapid and reasonable evacuation modelling in customized multi-layer building scenarios. A ControlNet is integrated to convert building floor plans into semantic feature maps, and a multi-level cellular automaton framework is constructed that includes floor layouts and bilateral stairwells, allowing to customize the number of floors and visualize dynamic evacuation process between staircases. Through comparative analysis with validated models and actual evacuation drill data, the proposed method demonstrates a higher semantic segmentation accuracy (IoU = 0.906) and more accurate evacuation time prediction (Error<9 %). Moreover, the proposed method automates the semantic interpretation of floor plans, enabling "image-to-simulation" automation and the generation of high-rise simulation scenarios directly from images within minutes, while effectively capturing the merging effect. The analysis also indicates that the number of stairwells and their internal width have a decisive influence on overall evacuation efficiency. This study aims to provide an efficient tool for the intelligent transformation of performance-based evacuation design and emergency management in high-rise buildings.

1. Introduction

With rapid urbanization, high-rise buildings have become a dominant form of urban infrastructure. Statistics indicate that such structures account for approximately 20 % of all buildings in China's developed cities, creating high-density built environments [1]. However, the extreme vertical height and complex layouts introduce severe risks. Recent studies have moved beyond general descriptions to quantify these specific mechanisms. Ivanov and Chow [2] utilized full-scale experiments to reveal the delays in vertical travel. Wang et al. [3] demonstrated how staircase geometry dictates bottleneck formation. Zhang et al. [4] emphasized the necessity of multi-scale spatial-temporal principles for global safety. Therefore, while ensuring evacuation safety is critical for urban resilience, it remains a formidable task due to the intricate coupling of these environmental and risk factors.

* Corresponding author.
** Corresponding author. Research Center for Smart Urban Resilience and Firefighting, Department of Building Environment and Energy Engineering, The Hong Kong Polytechnic University, Hong Kong.
E-mail addresses: yx.zhang@polyu.edu.hk (Y. Zhang), xy.huang@polyu.edu.hk (X. Huang).

https://doi.org/10.1016/j.jobe.2026.115441
Received 13 December 2025; Received in revised form 17 January 2026; Accepted 26 January 2026
Available online 29 January 2026

To navigate this complexity, one must address the fundamental challenges inherent to high-rise evacuation. The primary difficulties include long vertical distances, complex indoor environments, and huge crowd interactions [5]. Pioneering works by Proulx [6] and Kuligowski [7] have long established that these physical constraints are inextricably linked to human behavior, noting that pre-evacuation delays and decision-making processes are as critical as walking speeds. Occupants must navigate limited stairwells, which increases evacuation time and causes bottlenecks [8]. Peacock et al. [9] further demonstrated through empirical data that the interaction between pedestrian density and stairwell geometry significantly dictates movement speeds. Additionally, evacuation flows from different floors create complex merging behaviors in stairwells. As summarized in a recent review by Ivanov and Chow [10], these coupled complexities in modern indoor environments require more adaptive modelling approaches that can account for both physical and behavioral factors.

Crucially, evacuation safety is not solely determined by initial architectural design but is significantly influenced by ongoing facility management (FM). As highlighted by Ivanov et al. [11], the operational phase—including maintenance of egress routes, signage visibility, and changes in space utilization—plays a pivotal role in evacuation performance. Poor facility management can negate the benefits of a well-designed evacuation plan, creating unforeseen obstacles during actual emergencies. Therefore, an effective evaluation tool must be flexible enough to account for these dynamic spatial changes managed by FM teams.

Performance-based design (PBD) has become a standard engineering approach for addressing these safety challenges [12]. In assessing fire safety, the relationship between Available Safe Egress Time (ASET) and Required Safe Egress Time (RSET) is a critical determinant of evacuation safety [13]. ASET represents the duration during which the environment remains tenable for safe evacuation, with indicators such as temperature (<60 °C), CO concentration (<1000 ppm), and visibility (>10 m) measured at a height of 2 m above ground [14]. RSET, on the other hand, encompasses the total time occupants require to recognize, respond to, and evacuate to a safe area [15]. As defined in authoritative codes such as the *Code of Practice for Fire Safety in Buildings* in Hong Kong [16], PBD allows engineers to utilize computational simulation to demonstrate that the ASET is sufficient for all occupants to reach a place of safety before the onset of untenable conditions, typically quantified as RSET.

To achieve this, simulation methods are widely employed, which can be mainly divided into macroscopic models (Fluid dynamics models, etc.) and microscopic models (Social Force Models, Cellular Automaton, etc.) [17]. In the realm of microscopic modelling, Pelechano and Malkawi [18] significantly advanced the field by integrating psychological factors into agent-based models, demonstrating how human cognition affects route choice and evacuation efficiency. Due to computational efficiency, microscopic models are more widely used to study evacuation processes [19]. Tan et al. [20] proposed an improved SFM based on nuclear force theory for low visibility conditions. Li et al. [21] combined FDS with CA models to reproduce the Karamay fire evacuation. By overcoming experimental difficulties and ethical constraints, these simulation approaches have significantly advanced the understanding of pedestrian dynamics under coupled emergency scenarios [22].

However, current regulations on PBD often influence the focus of simulation studies. As outlined in standards like BS 7974 [23] and GB 50016 [24], the calculation of RSET is typically benchmarked against the time required to reach a protected exit (e.g., a stairwell enclosure). Consequently, much previous research has focused on evacuation within a specific floor. However, given the extreme vertical height of high-rise buildings, occupants remain in stairwells for extended periods, making safety within these areas equally critical [25]. Occupants evacuating downward from upper floors cause congestion for those on lower floors, which significantly slows the entire evacuation process [26]. Therefore, accurately capturing the merging effect of pedestrian flows between upper and lower floors is crucial for analyzing bottleneck formation and overall evacuation efficiency [27,28].

Commercial software such as Pathfinder has been widely utilized and validated for modelling such multi-floor evacuations and stairwell merging effects [29]. However, traditional simulation methods often require high programming skills or manual geometry definition. Converting complex scenarios into evacuation models is time-consuming and challenging [30]. Although established tools provide accurate results, the manual construction of simulation environments from raw floor plans remains a labor-intensive process, restricting the rapid iteration required in early-stage design [31]. For multi-story or high-rise buildings, the complex floor layouts and inter-floor relationships pose significant challenges to the efficiency of PBD works. With the development of computer technology, AI tools have been applied to assist in design conversion and evacuation prediction, providing new approaches for accelerating evacuation modeling and safety assessment [32,33].

The integration of deep learning offers a robust solution for automating the transition from architectural drawings to simulation-ready environments. ControlNet is an adapter-based neural network architecture designed to augment large-scale pre-trained diffusion models by incorporating task-specific spatial constraints [34]. Unlike standard generative models that may struggle with structural fidelity, it also maintains strict spatial consistency by learning the conditional mapping between edge maps, segmentation masks, or architectural sketches and their corresponding semantic features [35]. In the context of evacuation modelling, this allows for the precise extraction of topological relationships and wall-boundary constraints directly from raw floor plan images, which can effectively prevent the loss of geometric accuracy during the semantic interpretation phase, thereby ensuring that the resulting evacuation environment is high-fidelity [36].

This study proposes an extended cellular automata (CA) model for pedestrian evacuation modelling in high-rise buildings. Unlike traditional manual modeling approaches, this study integrates a ControlNet feature extraction module to automatically interpret semantic information from architectural floor plans and simplify the modeling of evacuation scenarios in the CA model. Meanwhile, a multi-floor CA framework for floor simulation is constructed, which can be extended to modules with any number of building floors according to specific engineering design needs. It simultaneously displays pedestrian evacuation within floors and between floors, which can provide multi-dimensional and comprehensive information for safety assessment, offering a theoretical basis and tool support for the development of intelligent performance-based design.

2. Methodology

2.1. Multi-layer building evacuation prediction framework

This work aims to achieve a rapid transition from multi-story building floor plans to pedestrian evacuation performance evaluation. The proposed technical framework consists of three main functional layers: (1) the user input layer; (2) the AI preprocessing layer; and (3) the evacuation simulation layer based on Floor Field Cellular Automata (FFCA), as shown in Fig. 1. In the user input layer, the number of floors is defined by the user, and corresponding building floor plans are provided as the initial material for the specific evacuation study.

The AI preprocessing layer uses the ControlNet deep learning model as the core technology, whose primary function is to convert building floor plans into semantic feature maps. This layer extracts key semantic information, such as walls, movable areas, and exits, from the original floor plan and encodes them into a standardized feature map format. Through this preprocessing step, complex architectural designs are distilled into feature maps with clear spatial attributes, providing standardized input for subsequent evacuation simulations.

The evacuation simulation layer is based on the extended Floor Field Cellular Automaton (FFCA) model and is responsible for executing the evacuation dynamic simulation of multi-story buildings. This layer receives semantic feature maps from the AI preprocessing layer, constructs cellular automaton grids for multiple floors, and simultaneously simulates horizontal evacuation within floors and vertical evacuation through stairwells, based on defined pedestrian movement rules and inter-floor interaction mechanisms. The simulation results include key safety indicators such as evacuation time, density distribution, and bottleneck locations, which provide comprehensive quantitative indicators.

These three functional layers are seamlessly connected through standardized data interfaces. The feature maps output by the AI preprocessing layer are directly mapped to the initial environment configuration of the FFCA model, ensuring an automated transition from design plans to evacuation simulations. The entire technical approach forms a complete closed-loop process, starting with the input of building floor plans, followed by AI-driven feature extraction, the generation of semantic maps, the construction of the FFCA model, evacuation simulation, and ultimately safety evaluation. which significantly enhances both the efficiency and accuracy of evacuation analysis for multi-story buildings.

2.2. AI architectural feature extraction

2.2.1. Database construction

To create floor feature maps that can be recognized and used by cellular automata, it is necessary to identify the architectural features to be studied. However, existing public datasets lack the specific semantic annotations required for vertical evacuation modeling. Therefore, a self-constructed dataset was built using a publicly available building floorplan dataset for training, which includes 34 floorplans of multi-story buildings, covering residential, office, and public buildings, with the number of floors ranging from 8 to 16 and varying building areas from 371.78 m^2 to 728.4 m^2.

The raw floor plans for the dataset were acquired from commercial repositories. Following collection, these data were manually screened to exclude samples that failed to meet unified design standards or exhibited structural redundancy. Subsequently, manual binarization was performed on the floor plans. This preprocessing focused on the building volume, movable areas, and exit information, as illustrated in Fig. 2. Through RGB feature mapping, the key architectural components were converted into binary maps, retaining only the core geometric information to serve as the ground truth for subsequent training.

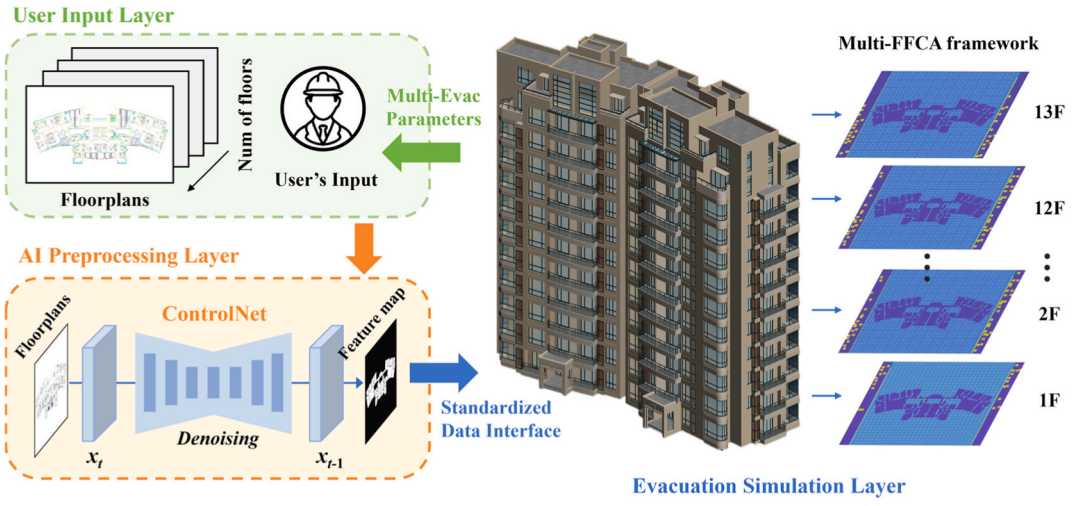

Fig. 1. Technical framework of the proposed multi-layer building evacuation prediction framework.

During the preprocessing, the original floor plans are standardized in size, adjusting all to a resolution of 512 × 512 pixels. Then, a combination of manual annotation and semi-automated segmentation is used to precisely label three key semantic elements in the floor plans: (1) Wall areas are marked with black pixels (0,0,0), representing impassable obstacles; (2) Movable areas are marked with white pixels (255,255,255), indicating areas where pedestrians can freely pass; (3) Staircase exit locations are marked with red pixels (255,0,0), representing evacuation exits; and (4) The specified ground floor exit locations are marked with green pixels (0,255,0).

To enhance the dataset's diversity and improve the model's robustness, four rounds of data augmentation are performed by rotating the annotated data 90° in succession, expanding the dataset to 146 multi-story training cases. Each sample pair consists of the original floor plan and its corresponding semantic map. The dataset is split into training (102 cases) and testing sets (44 cases) with a ratio of 7:3, which are used for model training, parameter tuning, and performance evaluation.

2.2.2. *ControlNet framework*

ControlNet is a conditional generation network based on diffusion models, which maintains the generation capability of pre-trained models while precisely controlling the spatial structure and semantic information of generated content [37]. Unlike training a network from scratch, ControlNet leverages the robust spatial priors of the large-scale pre-trained foundation model. This allows for efficient domain adaptation and accurate semantic segmentation even with a relatively smaller dataset, as the model primarily learns to align the specific semantic rules (e.g., color-coding) rather than learning geometric features from zero [38]. As shown in Fig. 3, the framework consists of two core stages: the training process and the inference process.

During the training process, ground truth data is first extracted from the dataset as input and encoded through an encoder to obtain initial feature representations. The encoded features then enter the forward process of diffusion, where Gaussian noise is gradually added to simulate image degradation. The forward diffusion network contains multiple neural network modules, with each layer receiving output from the previous layer and continuing to add noise. In this process, text prompts are injected as conditional information to guide the model in learning specific semantic features. The network calculates the difference between predicted noise (Pred noise) and actual added noise through a loss function. Mean squared error loss is used to optimize model parameters, enabling the model to accurately predict the noise added at each step.

During the inference process, the model receives a condition image as input and gradually removes noise through reverse diffusion to recover clear semantic segmentation maps. This process uses UNet architecture as the core denoising network, performing denoising operations through multiple iterations (Repeat times). In each iteration, the UNet network predicts the noise component of the current step and subtracts it from the image, progressively transforming random noise into meaningful semantic features. After a preset number of reverse diffusion steps, the decoder processes the denoised features and generates segmentation maps containing three semantic categories: walls, movable areas, and exits. This achieves accurate conversion from building floor plans to semantic feature maps.

The model training uses the AdamW optimizer with an initial learning rate of 1e-4 and a cosine annealing strategy for learning rate adjustment. Training is conducted on NVIDIA V100 GPUs with a batch size of 8 and 100 epochs. The number of reverse diffusion

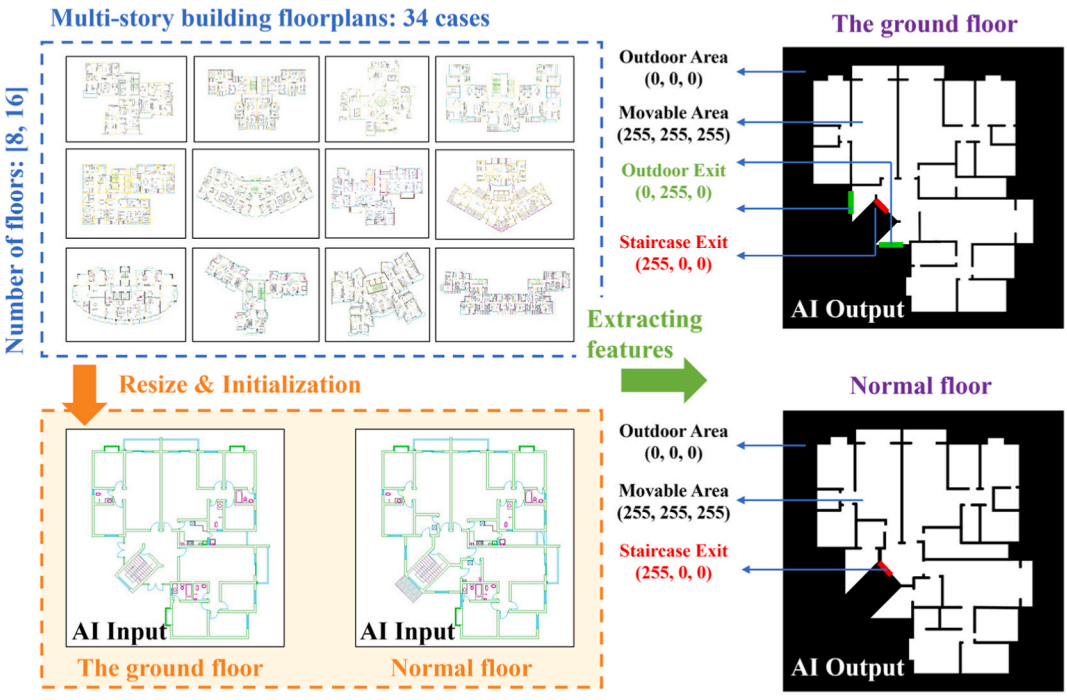

Fig. 2. Database construction of multi-floor building floor plans for ControlNet training.

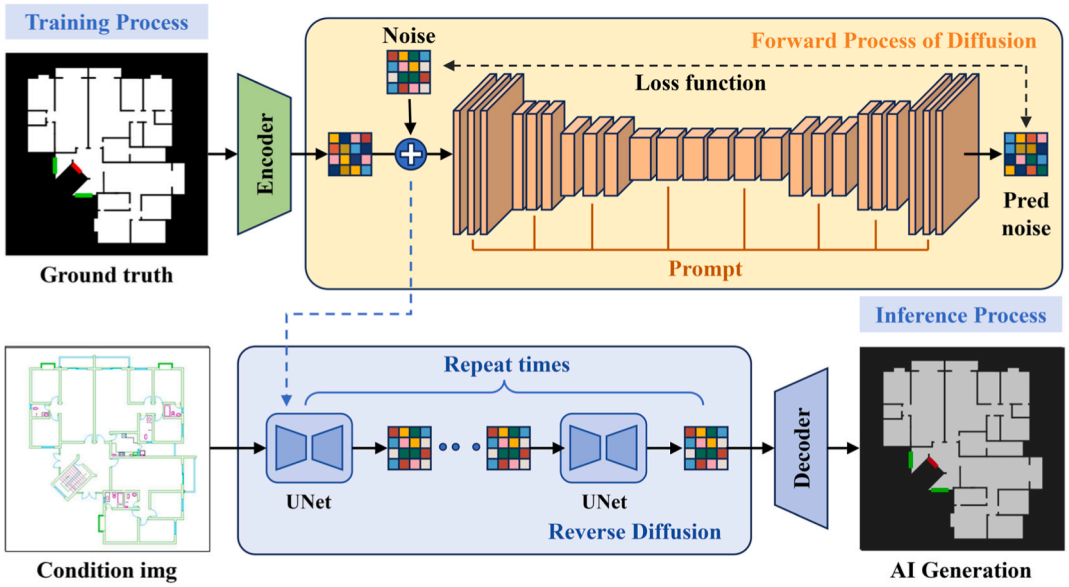

Fig. 3. Framework construction of ControlNet model.

iterations is set to 50 steps, balancing generation quality and inference efficiency.

2.3. Multi-layer evacuation FFCA model

In the context of evacuation model construction, FFCA, due to its high computational efficiency, low resource consumption, and scalability, is highly suitable for modeling inter-floor relationships in multi-story buildings and simulating synchronous evacuation across multiple floors and staircases. The following sections will provide a detailed description of the model assumptions, construction process, and parameter selection for the proposed FFCA.

2.3.1. Model assumptions

To facilitate analysis, this paper makes the following basic assumptions for the proposed cellular automaton, which ensure computational efficiency while capturing the core features of the evacuation process in high-rise buildings, providing a theoretical

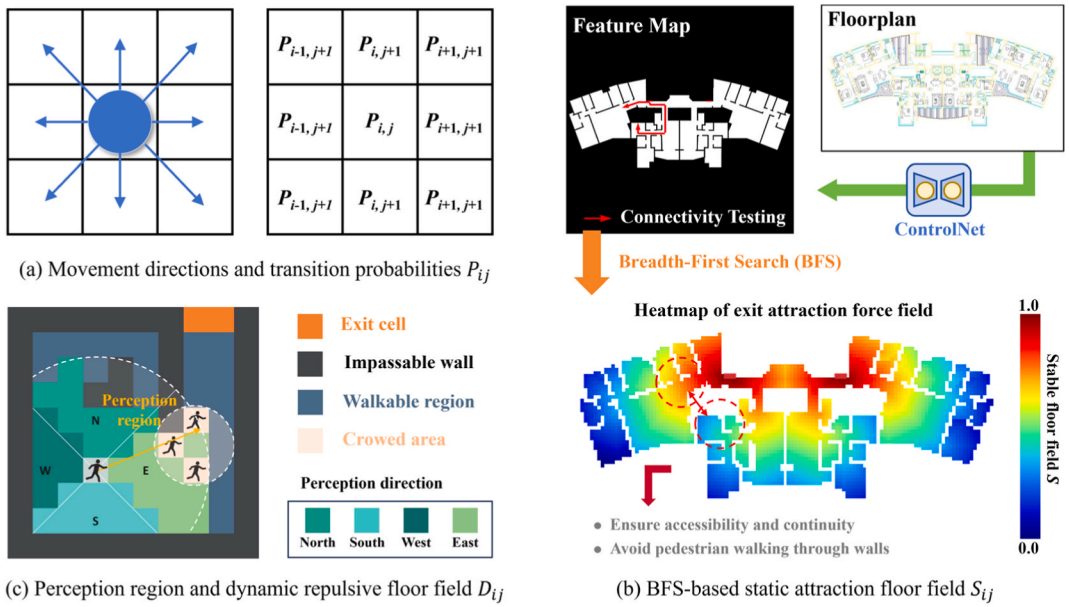

Fig. 4. Principle and calculation of pedestrian movement and transition probabilities of the proposed FFCA.

foundation for constructing a practical evacuation simulation system.

(1) Both space and time can be discretized. Space is discretized into regular rectangular grids, with each grid referred to as a cell; time is discretized into fixed time steps [22].
(2) All pedestrians are considered physically identical, each having an initial height of 1.70 m, shoulder width of 0.4 m, and weight of 60 kg, with an initial movement speed of 1 m/s [17].
(3) There are no psychological differences among occupants during evacuation, meaning complex psychological behaviors such as panic, herd effect, and competition are excluded [39].
(4) The evacuation process within staircases treats the staircase's helical structure as equivalent to a rectangle, with pedestrians moving in a single straight line. This simplification reduces the complexity of the spatial topology, facilitating unified modeling with the floor evacuation process.
(5) For the sake of simulation, the geometric parameters of the staircase follow the design standards of most high-rise buildings: a floor height of 4.0 m, including one intermediate landing platform and a stair width of 1.1 m [40].
(6) To focus on the movement dynamics and merging effects within high-rise evacuation, the pre-evacuation time (including detection and response time) is not considered in this work. All occupants are assumed to start their evacuation movement simultaneously at the beginning of the simulation ($t = 0$).

2.3.2. Pedestrian movement

As a typical discrete model, FFCA calculates the static attraction field of exits and the dynamic repulsion field between pedestrians. Together, these form the transition probability distribution of the entire evacuation scenario [17]. Pedestrians select their next movement direction based on the transition probabilities and move in one of the eight surrounding directions, simulating real evacuation behavior, which can be illustrated in Fig. 4 (a).

The transition probability P_{ij} for a pedestrian moving from the current cell (i,j) to an adjacent cell can be expressed as Eq. (1):

$$P_{ij} = N \cdot exp\left(k_S S_{ij} + k_D D_{ij}\right) \cdot \left(1 - \eta_{ij}\right) \tag{1}$$

Where N is a normalization coefficient, S_{ij} is the static floor field, representing the distance from the target cell to the nearest exit, reflecting the attraction effect of the exit on pedestrians. D_{ij} is the dynamic floor field, representing the distribution density of other pedestrians around the target cell, reflecting the repulsion effect between pedestrians. η_{ij} is the occupancy status of the target cell, with values of 0 or 1 indicating vacancy or occupation. k_S and k_D are the sensitivity coefficients for the static and dynamic fields, respectively, used to adjust the influence of each force field on pedestrian decision-making.

(1) Static floor field S_{ij}.

The static floor field represents the attraction of the exit to pedestrians, primarily based on the geometric distance from a cell to the exit. This study applies the Breadth-First Search (BFS) algorithm, which identifies the shortest path from each passable cell to the exit and can generate the global fields required for FFCA operations [41].

Compared to heuristic algorithms, BFS is inherently a flood-fill mechanism that propagates from the exit to calculate distances for all grid points in a single pass. In this work, defining that V represents the number of nodes (equivalent to the total number of cells, N_{cells}), E denotes the number of edges (approximately $E \approx 8V$ in an 8-neighbor grid), b is the branching factor, and d is the shortest path length. To generate a global field, the point-to-point algorithms like A* or JPS theoretically require searching each cell, resulting in a time complexity of $O\left(N_{cells} \cdot b^d\right)$. In contrast, the complexity of the traversal algorithm BFS is only $O(V + E)$, which can be simplified to $O(N_{cells})$ for grid maps with fixed connectivity. Therefore, BFS provides the highest efficiency for initializing static fields.

Since BFS propagates through passable areas until all reachable cells are covered, it provides accurate movement directions for pedestrians and avoids the wall-penetration issue in cellular automata. The application of the BFS algorithm is illustrated in Fig. 4 (b). Based on the shortest paths obtained via the BFS algorithm, the static floor field S_{ij} is calculated using Eq. (2) as follows:

$$S_{ij} = \max_{(i,j)}\left(\frac{1}{dist\swarrow(i,j)}\right) \tag{2}$$

Where $dist\swarrow(i,j)$ represents the shortest path from any given cell (i,j) to the nearest exit, calculated using BFS. The static floor field S_{ij} does not evolve over time and is inversely proportional to the distance from the exit. That is, areas closer to the exit exhibit a stronger attraction to pedestrians, reflecting their intention to locate the exit.

(2) Dynamic floor field D_{ij}

To reproduce the coupled effect between evacuees on different floors, a static floor field is considered to be updated in real-time based on the number of surrounding pedestrians, reflecting dynamic changes in pedestrian distribution. Its calculation considers the influence of other pedestrians within a certain range around the target cell:

$$D_{ij} = -\sum_{(m,n)\in\Omega} \frac{n_{mn}}{d+1} \tag{3}$$

Where Ω represents the neighbourhood with radius R centred on the target cell, corresponding to a pedestrian's perception range of crowding. n_{mn} denotes the occupancy state by other pedestrians of cell (i,j) within the neighbourhood. d is the Euclidean distance between the target cell and the neighboring cell, calculated as $d = \sqrt{(i_2 - i_1)^2 + (j_2 - j_1)^2}$. This formula indicates that pedestrians tend to avoid crowded areas and choose paths with lower density, which is shown in Fig. 4 (c).

Through parameter sensitivity analysis and calibration against previous data, the sensitivity coefficients were determined as follows: the static field sensitivity coefficient $k_S = 0.7$, highlighting the dominant role of exit attraction in pedestrian decision-making; the dynamic field sensitivity coefficient $k_D = 0.3$, reflecting pedestrians' tendency to avoid crowding; and the neighbourhood radius R is 4 cells (approximately 1.2 m), which aligns with the typical personal space requirement of pedestrians [42].

This work defines a single time step $\Delta t = 0.4\ s$, a cell size of 0.4 m × 0.4 m, and pedestrian movement speed on level ground is approximately 1.0 m/s. For stairwells, considering the reduced speed during descent, the velocity inside stairwells is adjusted to 0.7 m/s by modifying the relationship between cell size and time step.

At the beginning of each time step, all pedestrians are processed in random order for movement decisions. For each pedestrian, the transition probabilities for the eight surrounding neighboring cells are first calculated. A movement target is then randomly selected based on the probability distribution. If the target cell is already occupied or is an obstacle, the pedestrian remains in place and will attempt to move again in the next time step.

When a pedestrian moves to an exit cell, it is considered to have completed the evacuation of the current floor. The evacuation time is recorded and the pedestrian will be transferred to the corresponding stairwell based on the exit location to continue vertical evacuation, or exit the system directly if on the ground level. The total evacuation completion time is defined as the total duration from the start of the simulation until all the pedestrian have completed their evacuation. It should be noted that this value only represents the movement time within the RSET framework.

2.3.3. Evacuation scenario construction

As mentioned in section 2.2.2 above, the architectural features of floor plans will be extracted through a ControlNet module. And then, the generated feature map would be transferred to FFCA to construct the evacuation environment. Hence, A dictionary needs to be defined between feature maps and the corresponding cell property values, which is shown as Table 1.

First, during the processing of the semantic map generated by ControlNet, the HSV color space method is applied to identify pixels, thereby enabling accurate color recognition and classification. Next, for each cell-corresponding image region, the mean RGB value of all pixels within the region is calculated. The region is then classified according to the predefined color category with the closest match, improving the accuracy of semantic segmentation.

After the mapping process, further spatial processing is required to meet the requirements of the FFCA model. First, a connectivity check is performed on the transformed cellular grid to ensure that all movable areas have reachable paths to the exits. Second, ID assignment and indexing are conducted for exit cells to facilitate subsequent evacuation flow statistics and stairwell allocation. Finally, a wall cell layer is automatically added around all movable areas to prevent pedestrians from moving into undefined regions. The processed cellular grid matrix is then directly used as the initial environmental input of the FFCA model without manual intervention.

2.3.4. Multi-floor CA framework

A predefined framework for constructing an extended cellular automata model of multi-story buildings is established, which consists of three cellular regions *Grid* 1, *Grid* 2, and *Grid* 3, with dimensions of 11 cells × 125 cells, 125 cells × 125 cells, and 11 cells × 125 cells, respectively. Hence, a cellular automaton interface with a total size of 147 × 125 cells is built, which can be seen in Fig. 5 (a).

These cellular regions serve various functions: (1) *Grid* 2 represents the horizontal architectural plane from a top-down view, used to simulate the evacuation process within each floor moving toward indoor exits; (2) *Grid* 1 and *Grid* 3 represent the vertical stairwell regions, used to simulate pedestrians' vertical movement between floors. All the pedestrian evacuation processes within each cell region share the same time step.

The size of each cell in *Grid* 2 is defined as 0.4 m × 0.4 m, representing a total canvas of 50 m × 50 m to adapt to most architectural floor layouts. In *Grid* 2, each pedestrian occupies one cell and can move at most one cell per time step. Therefore, the pedestrian walking speed is defined as 1.0 m/s.

In *Grid* 1 and *Grid* 3, to unify the scaling and sizes of staircases and the horizontal floor area, the size of each cell is defined as 0.13 m × 0.13 m *Grid* 1 and *Grid* 3 are equivalent to rectangular areas with a projected length of 16.6 m. Each pedestrian occupies nine cells,

Table 1
Mapping relationship between pixel features and corresponding cell property values.

Pixel colores	Feature	Cell value	Description
(0, 0, 0)	Outdoor area and wall	1	Impassable entity
(255,255,255)	Available indoor area	0	Available for pedestrian movement
(255, 0, 0)	Staircases exit	3	After passing through, proceed to the stairwell rather than the outdoor area
(0, 255, 0)	Outdoor exit	8	Reach the outdoor area and complete evacuation

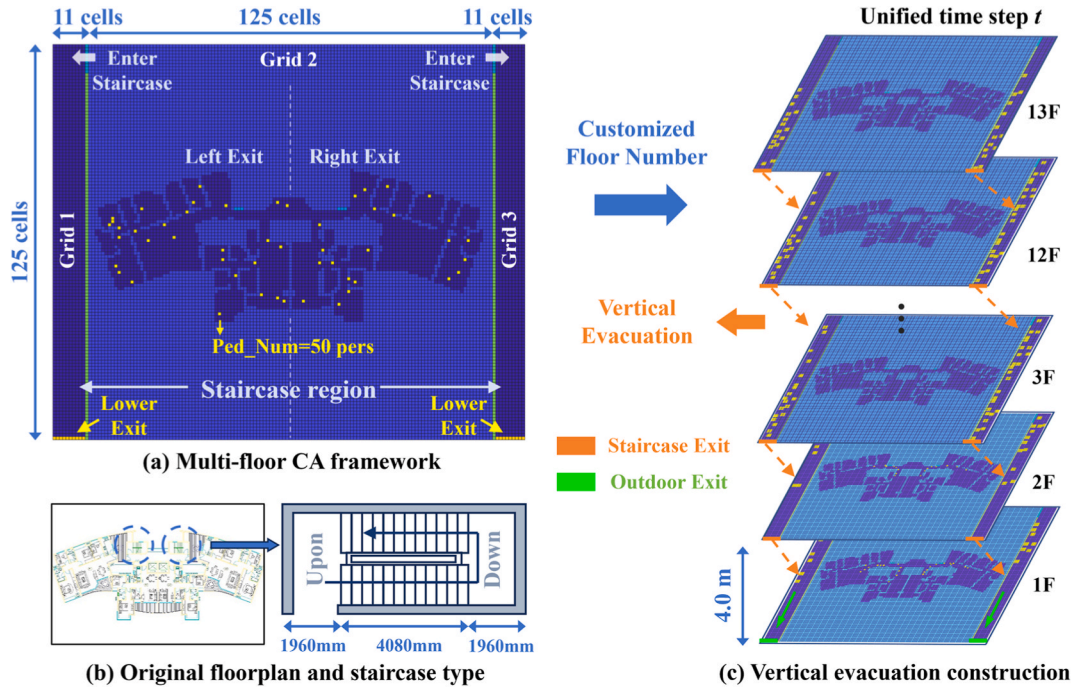

Fig. 5. Predefined framework for multi-floor building evacuation modelling using FFCA.

and correspondingly, the pedestrian can move within the range of the remaining nine surrounding cells in any of the eight directions per time step.

The actual staircase structure is considered in Fig. 5 (b). The total length of the steps is 4.08 m, and each landing has a length of 1.960 m. Based on the macroscopic assumptions described in Section 2.3.1, the loop-shaped staircase structure is unfolded into a vertical rectangle, resulting in a total projected staircase length of 12 m. Combining the projected cell length and the actual staircase length, the average descending speed of pedestrians in the staircase is defined as $v = 0.7$ m/s, which meets the SFPE correction factor of 0.68 for downward evacuation speed. In summary, the different cell regions and the corresponding pedestrian movement speeds are presented in Table 2.

During the evacuation simulation, the following definitions are applied: when a pedestrian evacuates through the left-side exit along the central axis of *Grid* 2, the pedestrian is counted as n_{left} and enters *Grid* 1, which represents the left staircase. Conversely, when evacuation occurs through the right-side exit, the pedestrian is counted as n_{right} and enters *Grid* 3, which represents the right staircase. This process can be seen in Fig. 5 (c).

To handle the transition between grids with different cell sizes, a logical mapping interface is established. The staircase entrances function as a state-check gate. When a pedestrian at the exit of *Grid* 2 (occupying 1 cell) attempts to enter *Grid* 1 or *Grid* 3, the model checks the occupancy of the corresponding entrance area (mapped to a 3×3 cell block) in the stairwell grid. If the target 3×3 area in the stairwell is vacant, the agent is transferred from *Grid* 2 to *Grid* 1 and *Grid* 3 and is instantly redefined to occupy 9 cells. This mechanism ensures seamless connectivity while utilizing the finer grid resolution (0.13 m) in stairwells to naturally simulate the reduced descent speed (approximately 0.7 m/s) and constrained movement space.

In this work, all evacuation cases are repeated 30 times, and the simulation results are averaged. By constructing the described single-layer cellular automaton framework, users can flexibly define the number of floors in the studied multi-story building. This framework allows simultaneous observation of horizontal evacuation on each floor and vertical evacuation within staircases during the same simulation period. After the simulation, the model can output the evacuation time for each floor, the occupancy status within staircases, and the corresponding dynamic distribution of evacuation density. These results provide comprehensive data for engineers conducting performance-based evacuation safety design.

Table 2
Size of each cell region and corresponding pedestrian moving speed within region.

Region	Cell size(m)	Grid size(cells)	Region size(m)	Ped size(cells)	Speed(m/s)
Grid 1	0.13 × 0.13	11 × 125	1.43 × 16.25	3 × 3	0.7
Grid 2	0.40 × 0.40	125 × 125	50 × 50	1 × 1	1.0
Grid 3	0.13 × 0.13	11 × 125	1.43 × 16.25	3 × 3	0.7

3. Results and analysis

3.1. Performance of feature extraction

To validate the effectiveness of the ControlNet module in semantic segmentation of architectural floor plans, this work compares it with two classic image transformation models: the baseline Generative Adversarial Network (GAN), the Pix2Pix model with the U-Net as the generator structure, and the discriminative segmentation model SegFormer. A total of 44 architectural floor plans from the test set are used to evaluate the semantic segmentation performance of multi-story floor plans from a quantitative perspective. Hence, three standard metrics are employed: (1) Intersection over Union (IoU); (2) Pixel Accuracy (PA); (3) F1 score, which is the harmonic mean of precision and recall. The evaluation results for these three metrics are shown in Table 3.

As shown in Table 3, the proposed ControlNet outperforms not only generative baseline models (GAN, Pix2Pix) but also the discriminative segmentation model (SegFormer). This is because the Transformer architecture of SegFormer requires massive training samples, making it prone to overfitting with limited datasets and unable to capture fine-grained structural details. In contrast, the base parameters of ControlNet are pre-trained on large-scale datasets; thus, the IoU = 0.906 verifies that framing this task as a conditional generation problem can fully leverage the robust spatial prior knowledge of pre-trained diffusion models, effectively reconstructing the structural details missed by purely discriminative models, which ensures the correct transition and mapping from the architectural floor plan to the FFCA model.

3.2. Effectiveness validation of the FFCA model

Due to the objective limitations of conducting comprehensive verification evacuation experiments in high-rise buildings, this study adopts a multi-tiered strategy to verify the reliability of the proposed FFCA model. The framework is validated by comparing its output results with peer-validated simulation models, industry-standard commercial software (Pathfinder), and real evacuation drill data from the Hong Kong Polytechnic University (PolyU). This comprehensive cross-validation covers both theoretical consistency and practical applicability.

3.2.1. Validation with the previous evacuation simulation model

As the FFCA modeling process involves several macro assumptions and model parameters, the validity of the modeling parameters is tested with a multi-layer evacuation model from Zeng et al. that has been experimentally validated, as shown in Fig. 6 [43]. The evacuation case of Zeng et al. was selected from an 11-story high-rise office building in Zhejiang, China, where the floor layouts were similar across levels and were omitted. The stairwell consisted of 8 stair sections, with each step having a height of 0.16 cm and a length of 0.28 cm. In the validation experiment, 150 employees of the office building participated in the evacuation drill.

Fig. 6 demonstrates that the proposed FFCA model produces evacuation simulation results that closely align with those of Zeng et al.'s model for a high-rise building scenario. The evacuation time for the proposed model is 210.8 s, while Zeng et al.'s simulation results show 224 s, a slight difference with an error of approximately 6 % [43].

Preliminary analysis suggests that the simplification of the stairwell structure to a vertical rectangular shape in this study may be the reason for the discrepancy. In the actual evacuation process, each section of the stairwell contains two horizontal platforms, and the horizontal distance between them, especially in high-rise buildings, has a significant overlapping effect that cannot be ignored. Therefore, the actual travel distance in the evacuation scenario designed by Zeng et al. is slightly larger than that in the proposed model. However, considering the safety factor of 1.5–2.0 in evacuation time evaluation, the model error is acceptable.

Fig. 7 compares the proposed model with a Pathfinder simulation of a high-rise dormitory evacuation from Deng et al. [44]. Pathfinder is a widely verified commercial software used to simulate multi-story evacuation and the merging effect in stairwells [29]. Fig. 7 (a) shows the simulation scenario, in which the building has 20 floors with 18 rooms on each floor, 100 occupants are evenly distributed on every level, and the complete structure of stairwells and landings is retained. As shown in Fig. 7 (b), occupants need to move downward along the spiral stairs to complete their evacuation.

Fig. 7(c) compares the evacuation times of occupants on the middle floors. As Assumption 4 simplifies the spiral stairwell into a vertical rectangular structure, the geometric constraint of landings and the friction caused by turning movements are inevitably neglected. Consequently, the proposed model yields shorter escape times compared to Pathfinder, indicating a smoother evacuation process, and the relative difference for the five selected floors ranges from 11.3 % to 17.2 %.

Although explicitly representing landings could reduce this discrepancy, it would significantly complicate the automated modeling process. Given the common safety factor of 1.5–2.0 in PBD tasks, this 11–17 % overestimation of flow rate falls well within the safety

Table 3
Architectural feature extraction performance of three mainstream models.

Model	IoU			Average IoU	PA	F1
	Wall	Exit	Available area			
GAN	0.734	0.573	0.762	0.690	0.826	0.771
Pix2Pix	0.801	0.692	0.819	0.771	0.862	0.833
SegFormer	0.825	0.710	0.853	0.796	0.845	0.851
ControlNet	0.919	0.860	0.939	0.906	0.876	0.887

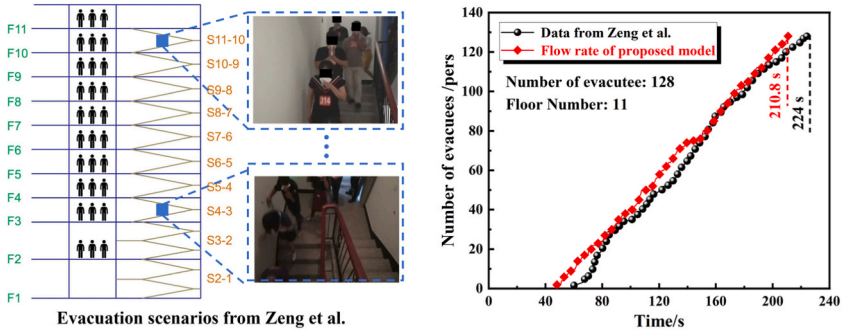

Fig. 6. Comparison of evacuation simulation results between the proposed model and those from Zeng et al. [43].

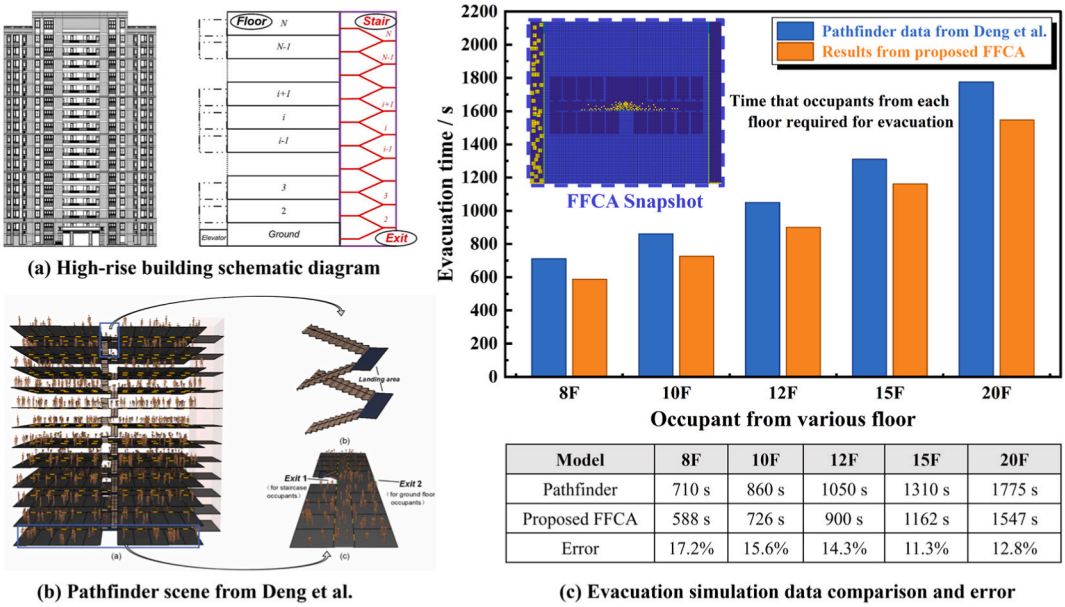

Model	8F	10F	12F	15F	20F
Pathfinder	710 s	860 s	1050 s	1310 s	1775 s
Proposed FFCA	588 s	726 s	900 s	1162 s	1547 s
Error	17.2%	15.6%	14.3%	11.3%	12.8%

(c) Evacuation simulation data comparison and error

Fig. 7. Comparison of evacuation simulation results between the proposed FFCA model and Pathfinder from Deng et al. [44].

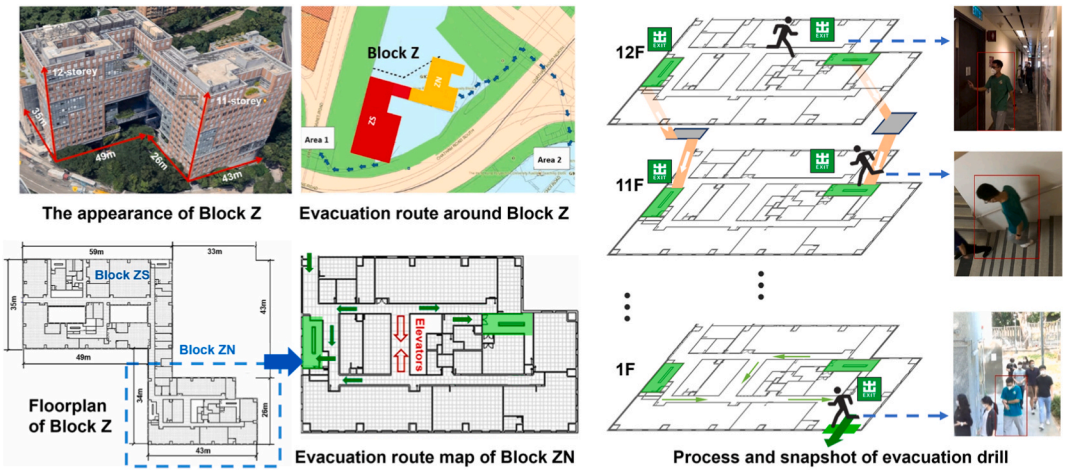

Fig. 8. Evacuation scenario and drill settings of Zhang et al. in the Hong Kong PolyU [45].

margin. Thus, for the purpose of rapid design iteration, this error is considered acceptable.

3.2.2. Validation with the previous evacuation simulation model

To further validate effectiveness, a comparison is conducted between the proposed framework and an evacuation drill from Block Z at the Hong Kong Polytechnic University (PolyU) organized by Zhang et al. [45]. The detailed drill plan, participants, and evacuation routes are shown in Fig. 8.

The Block Z of PolyU is a 12-story multi-functional high-rise building with a total floor area of 46,000 m^2. Each floor of the building is divided into two main zones: Block ZN and Block ZS. The drill mainly focused on the evacuation process in Block ZN, and there were more than 800 participants. During the drill, elevators on each floor were prohibited, and all occupants were required to evacuate vertically through stairwells [45].

Based on the Block ZN floor plan from Zhang et al., a 12-story evacuation simulation scenario was constructed using the proposed FFCA framework, with an average of 70 occupants per floor (840 total). The simulated average evacuation time per person and standard deviation are shown in Table 4.

Under the proposed FFCA framework, the average evacuation time per person was 505.73s with a standard deviation of 320.03, showing a 9 % difference from the experimental data of Zhang et al. [45]. Analysis of the original study suggests that this difference is attributed to the lack of serious and active attitudes among many evacuees during the drill. Compared to real emergencies, the drill evacuees had lower desired speeds. Meanwhile, many evacuees spontaneously formed groups, with frequent waiting for each other, which delayed the evacuation process. With these factors, the per-person evacuation time obtained from the proposed model demonstrates sufficient rationality and interpretability.

Additionally, due to the common difficulties in organizing participants and recording data during evacuation, the original study did not provide corresponding data on flow rates at different staircases, evacuation completion times for each floor, or evacuation times within staircases. In contrast, the proposed FFCA framework can not only record overall and per-person evacuation times but also capture flow data at different staircases and floor levels, while displaying the dynamic evacuation process, as shown in Fig. 9. These data can serve as an effective supplement for engineers and designers to comprehensively assess evacuation safety.

The comparisons mentioned above demonstrate that the FFCA model maintains an acceptable consistency with both established theoretical models and empirical drill data. Given the complexities of high-rise dynamics, such an error margin (e.g., from structural difference and human factors) is well within the acceptable range for PBD tasks, confirming that the model remains a robust tool for safety assessment when large-scale experimental data are scarce. The following text will delve into a case study to further discuss the performance of the proposed model in simulating high-rise building tasks.

3.3. Simulation practice and performance analysis

A typical office building from the test set is selected as an example to analyze the simulation performance and parameter sensitivity. Fig. 10 shows the floor plan of the selected building and the feature extraction process of the pre-trained ControlNet engine, followed by simulation using the multi-storey FFCA framework. The building dimensions are 33 m × 17 m, with a useable area of approximately 528.17 m^2. The building has 10 floors, with each floor having 2 staircases (entrance width of 1.1 m) and 6 offices, a floor-to-floor height of 4 m, and a preliminary occupancy of 50 people per floor. All occupants evacuate simultaneously from their respective floors and use the 2 staircases for vertical evacuation. After reaching the first floor, they exit the evacuation scenario through the first-floor exit.

Fig. 10 focuses on the floor regions represented by *Grid* 2 and shows the evacuation evolution process at different floors through curves of remaining occupants over time on each floor. Since the ground floor receives occupants from other floors, the figure plots evacuation curves for all floors except 1F for convenient comparison. As mentioned in Section 2.3.2, due to the repulsive force between occupants, under the influence of the merging effect, occupants on upper floors can enter the staircases faster than those on lower floors. Meanwhile, the evacuation curve for occupants on 10F is smoother because there is no merging effect from upper-floor occupants. For occupants on lower floors, the evacuation curves show a significant platform-type pattern, which is attributed to the repulsive force from occupants evacuating vertically from upper floors in the staircases, causing them to remain longer at the staircase entrances. This results in occupants on higher floors being able to leave their floors faster, while occupants on lower floors require relatively longer evacuation times. In terms of the relative rate represented by the slope of evacuation curves, for the upper floors from 10F to 5F, the lower the floor, the slower the evacuation rate on the floor plane; however, after reaching the peak, for the lower floors from 5F to 2F, the lower the floor, the higher the evacuation rate on the floor plane.

Fig. 11 shows the pedestrian flow data for the downward staircases on both sides of each floor, which has been smoothed with an alpha of 0.8 for convenient observation. The length of the *x*-axis interval spanned below each curve represents the staircase utilization rate, which reflects the retention of evacuees in the staircase, and the curve endpoints also characterize the evacuation completion time of each floor.

Table 4
Comparison of evacuation time between the proposed model and that from Zhang et al. [45].

Source	Evacuees (pers)	Average Evac_time	Standard deviation (SD)
Zhang et al. [45]	>800	553s	405s
Proposed model	840	505.73	320.03

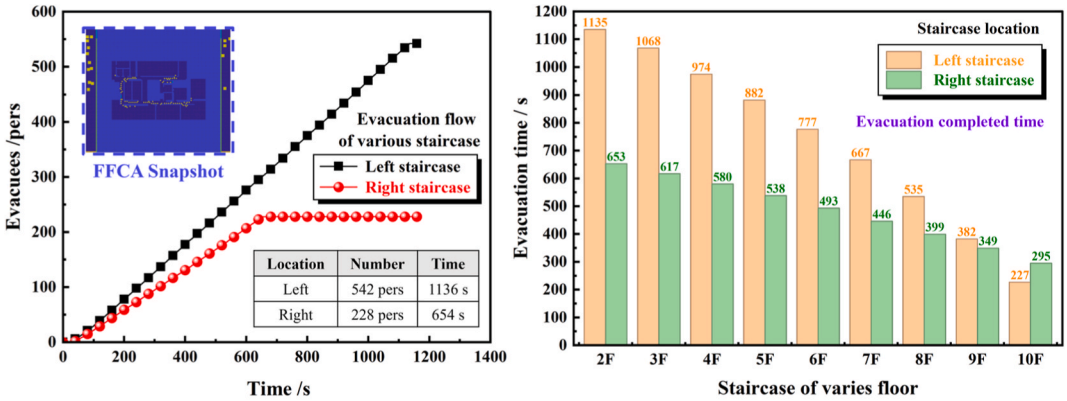

(a) Evacuation flow rate of various staircase location (b) Evacuation completed time of staircase under various floors

Fig. 9. Evacuation flow rate and evacuation completed time of staircases under different locations and floors simulated by the proposed FFCA framework.

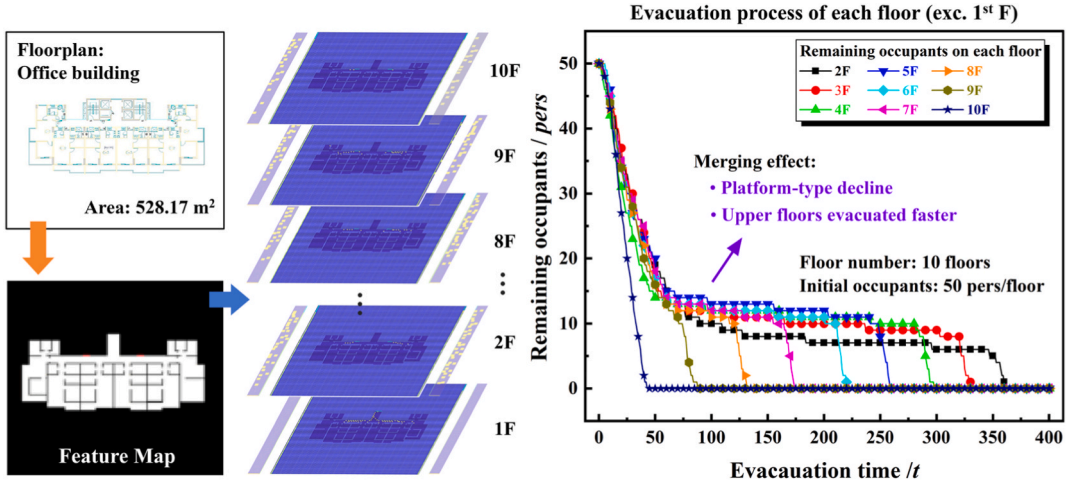

Fig. 10. Modelling and the evacuation process versus time of each floor.

Since there are no occupants from upper floors, the downward staircases of 10F are only used by 10F occupants for vertical evacuation. Therefore, the usage time of the downward staircases of 10F is 68s, with a peak of approximately 12 people in a single staircase. As the floor descends, the usage time and evacuation completion time of the downward staircases on lower floors gradually increase. Since the positions of the left and right staircases in the input scenario are symmetric, the trends of the two curves are approximately the same. For the peak number of evacuating occupants in a single staircase, in the upper floor interval from 10F to 5F, the single-side peak slowly increases to approximately 16 people, while in the subsequent interval from 5F to 2F, it slowly decreases to 11 people, which corresponds to the phenomenon observed above.

3.3.1. Staircase entrance width

To further analyze parameter sensitivity and demonstrate the advantages of the proposed model in optimizing the PBD task, the staircase door width is subsequently adjusted to 0.9 m and 2.6 m to further study the impact on evacuation efficiency. 0.9 m represents the minimum staircase entrance size in many building fire design codes [21], while 2.6 m is the maximum entrance width obtained by removing the staircase enclosure wall in the building drawings.

Fig. 12 shows the total evacuation time and the evacuation completion time for each floor under different stairwell entrance widths. Fig. 12 (a) indicates that the stairwell entrance width has a slight impact on the total evacuation time of the building. When the entrance width w increases from 0.9 m to 1.1 m, the evacuation time slightly decreases, as a wider stairwell optimizes pedestrian flow into the stairwell. However, further increasing the entrance width results in a noticeable marginal decrease in evacuation time. Even with a fully open stairwell ($w = 2.6$ m), overall evacuation time decreases by only 2 s and no longer correlates with stairwell entry width, or floor-level exit width.

Fig. 12 (b) also indicates that under different stairway entrance widths, the evacuation time within the stairway only slightly decreases or remains almost unchanged. This phenomenon leads to the conclusion that, in high-rise building evacuations, the

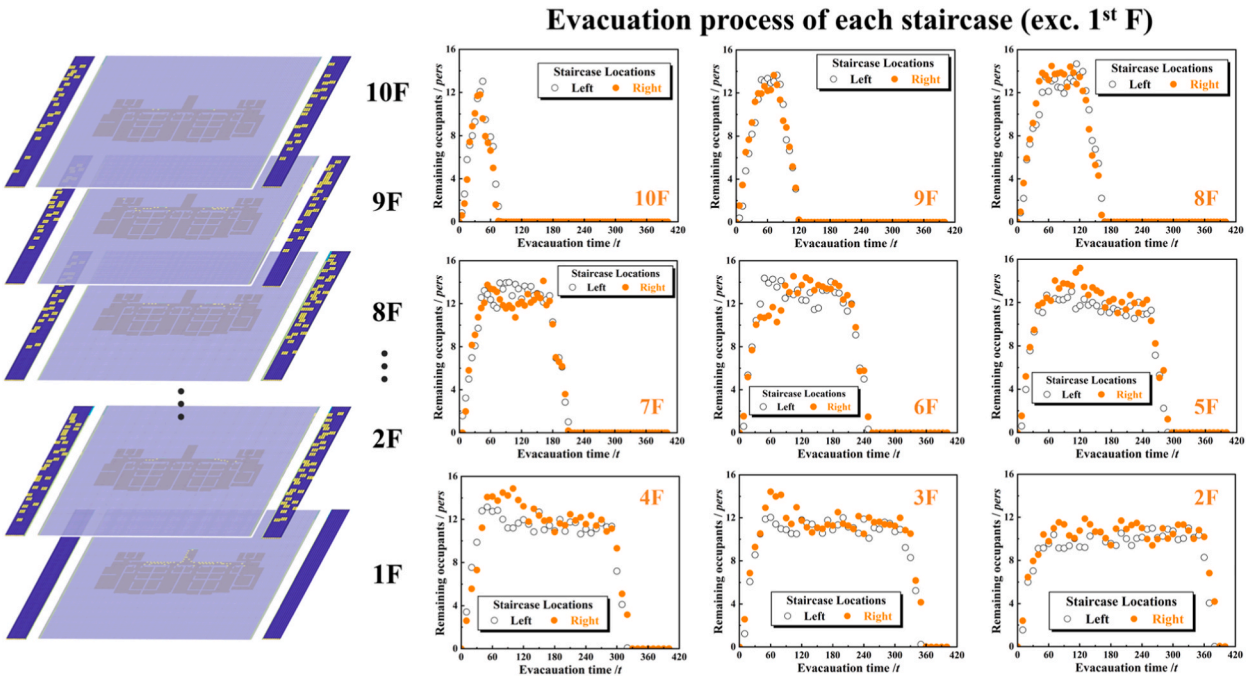

Fig. 11. Evacuation process versus time of each staircase under different floors.

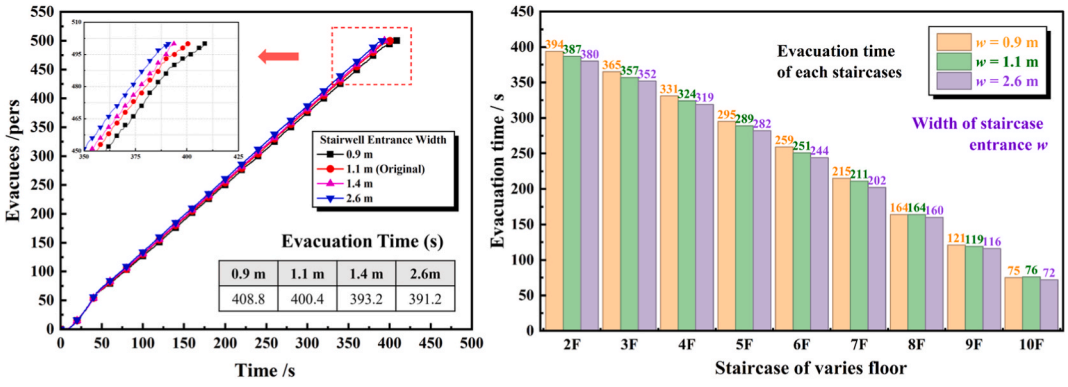

(a) Evacuation efficiency of various staircase entrance widths (b) Evacuation completed time of staircase in various floors

Fig. 12. Total evacuation efficiency and evacuation completed time of each floor under various staircase entrance widths (w = 0.9 m, 1.1m, and 2.6m).

evacuation within floors is not the primary factor affecting overall evacuation efficiency. Many previous studies have similarly pointed out that, during high-rise evacuations, the time spent by pedestrians within the stairway is significantly greater than the time spent evacuating between floors [46]. The vertical evacuation process in high-rise buildings is notably different from the horizontal evacuation pattern between floors, which also suggests that many prediction studies that only consider single-floor evacuation scenarios are somewhat one-sided [32].

3.3.2. Number of staircases

To explore the main factors influencing the overall evacuation, the number of stairways in the current evacuation scenario is further adjusted from two exits (left and right) to a single stairway on the left side, which is equivalent to halving the width of the downward stairs within the stairway.

Fig. 13 shows a comparison of the overall evacuation time and evacuation completion times for each floor between the evacuation scenario with a single left stairway and the original evacuation scenario. Fig. 13 (a) indicates that when there is only a left-side stairway, the overall evacuation time significantly increases from 400.4 s in the original scenario to 755.6 s. Fig. 13 (b) also shows that the presence of only a left-side stairway greatly extends the evacuation completion times for each floor and significantly hinders

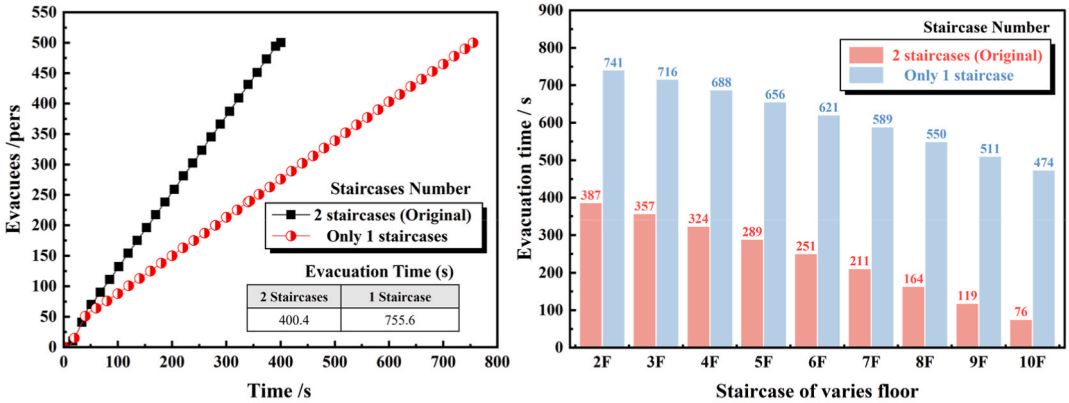

(a) Evacuation efficiency of various staircase entrance widths (b) Evacuation completed time of staircase under various floors

Fig. 13. Comparison of evacuation efficiency and evacuation completed time of each floor under various staircase numbers (Original two staircases and only one staircase).

the evacuation on the 10th floor, which has no other pedestrians from upper floors.

3.3.3. Initial occupant distribution

The initial number of pedestrians on each floor significantly affects the overall evacuation of high-rise buildings. To investigate this impact, different initial numbers were set for odd and even floors while the total number of pedestrians ($N = 500$) was kept constant. The ratio of initial pedestrians on odd and even floors is defined as k, and the predicted results for $k = 1{:}1$, 1:2.3, and 1:4 are shown in Fig. 14.

Fig. 14 (a) indicates that the total evacuation time increases as the ratio k decreases. Meanwhile, the time spent within the stairway also increases slightly in Fig. 14 (b). Using a sample of 10F and 9F, attributing to the merging effect, when the occupant proportion on upper floors is larger than that of adjacent lower floors, bottleneck congestion in front of the stair entrances of lower floors is intensified, which causes the occupants on lower floors to require more time to enter the stairway.

To better demonstrate the merging effect, Fig. 15 uses alternating ratios (k = 1:1, 2.3:1, and 4:1), ensuring the top floor has a smaller initial number of pedestrians. It also indicates that as the ratio k increases, both the total evacuation time and the time spent in the stairway decrease. This indicates that the merging effect originates from the top floor. Fewer initial occupants on the top floor will lead to earlier clearance of the upper stairway, which reduces the congestion on lower floors, and the bottleneck in front of the staircase

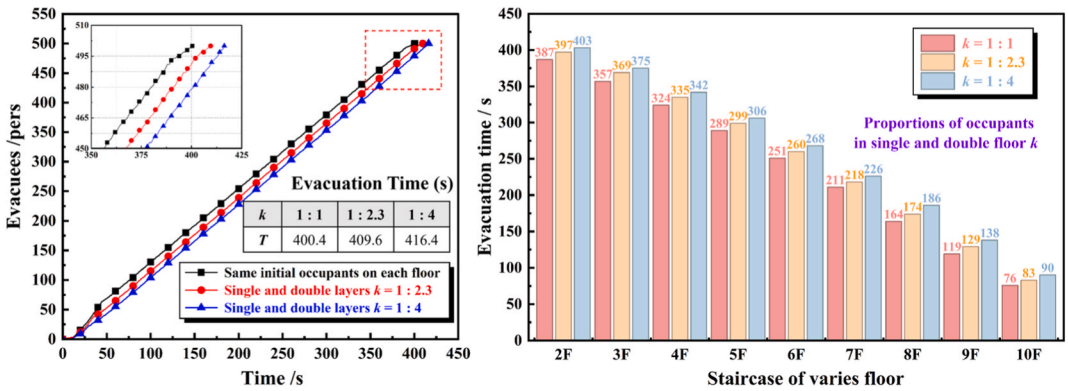

(a) Evacuation efficiency of varies occupant proportions (b) Evacuation completed time of staircase in various floors

Fig. 14. Comparison of evacuation efficiency and evacuation completed time of each floor considering different initial density ($k = 1{:}1$, $k = 1{:}2.3$, $k = 1{:}4$).

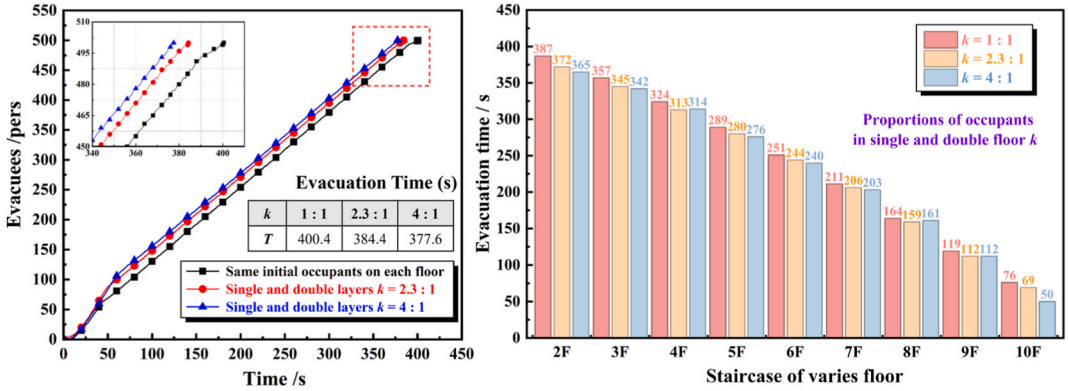

(a) Evacuation efficiency of varies occupant proportions (b) Evacuation completed time of staircase in various floors

Fig. 15. Comparison of evacuation efficiency and evacuation completed time of each floor considering different initial density (k = 1:1, k = 2.3:1, k = 4:1).

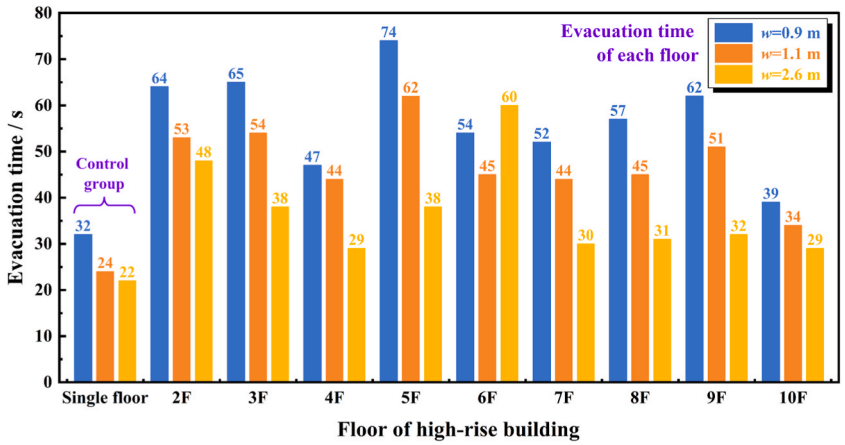

Fig. 16. Comparison of evacuation time of the single floor and high-rise building under different stairway entrance widths (w = 0.9 m, 1.1m, and 2.6m).

entrance is weakened, resulting in a shorter total evacuation time.

3.3.4. Merging and bottleneck effects

The proposed conclusion that entrance width has minimal impact on internal stairway evacuation time does not contradict existing research identifying exit width as a key bottleneck factor. To quantify the interaction between the merging effect and bottleneck congestion, Fig. 16 compares evacuation times for each floor under different entrance widths, using a single floor as a reference. The evacuation time here is defined as the duration required for occupants to completely enter the stairway and leave their floor, which quantifies the bottleneck effect to a certain extent.

Fig. 16 shows that, for single-floor evacuation, clearance time decreases as the stairway entrance width increases, indicating that the bottleneck effect weakens. However, in multi-floor scenarios, the bottleneck is also influenced by the merging effect. Occupants are repelled by those descending from upper floors, causing prolonged congestion at the entrance that varies by floor level. Although the bottlenecks on each floor are alleviated as the entrance width increases, the convergence effect exacerbates congestion in front of the exit, even on the top floor, and this phenomenon is more pronounced on lower floors.

Macroscopically, the bottleneck delay constitutes a minor portion of the process, as the majority of the time is the vertical movement within the stairway. High-rise evacuation comprises two modes: horizontal evacuation from floors to the stairway, and vertical evacuation within the stairway. Although the merging effect slightly intensifies bottleneck congestion, the overall evacuation time is still dominated by vertical movement. Consequently, while the stairway entrance width affects congestion levels, its impact on the total evacuation time is minimal, which also explains the conclusion in Section 3.3.1. Hence, when engineers and designers conduct performance-based safety assessments, they must not only consider the entrance width to the stairway on each floor, the initial occupant distribution, but also comprehensively account for the number and orientation of stairways, as well as the width of the downward stairs.

4. Conclusions

This study addresses the key challenges of evacuation safety assessment in high-rise buildings by developing an intelligent evacuation modeling framework that integrates ControlNet and an extended cellular automaton (CA) model. This framework enables engineers to rapidly and accurately conduct performance-based evacuation safety evaluations. The ControlNet achieves precise feature segmentation of building characteristics, while the multi-level CA framework achieves the simultaneous simulation of horizontal evacuation within floors and vertical evacuation in stairways. This allows for the customization of the number of floors while effectively capturing the merging effect in high-rise building evacuation. Through comparative analysis with actual evacuation drill data, the proposed model demonstrates high semantic segmentation accuracy (IoU = 0.906) and precise evacuation time prediction (error <9 %).

Through systematic analysis, the study quantifies the dominant role of stairway configuration and the initial occupant distribution in overall evacuation efficiency, emphasizing that the staircase width plays a decisive role in the high-rise evacuation process. While the entrance size of the stairway has a significant impact on single-floor horizontal evacuation time, it is not a primary factor in high-rise evacuation due to the merging effect. Rather than merely addressing the capability gap, this work provides an efficient automated tool to supplement current PBD tasks. It overcomes the labor-intensive modeling process of traditional methods, offering theoretical support for promoting the intelligent transformation of performance-based evacuation design and emergency management in high-rise buildings.

Although the current model demonstrates high accuracy on the test set covering residential, office, and public buildings, the dataset size remains a limitation. Future work will focus on expanding the dataset in terms of scale and the types of buildings included, improving the accuracy of ControlNet in extracting key architectural features, and conducting further experiments to validate and optimize the parameters of FFCA. This work will also consider incorporating stochastic pre-evacuation time distributions to further enhance the model's comprehensiveness for various emergency scenarios. Additionally, a user-friendly GUI system will be developed to allow users to easily implement and quickly carry out customized tasks. Furthermore, the integration of big data and Internet of Things (IoT) technologies will be explored to build a digital twin system, enabling real-time, rapid, and accurate modelling and prediction of high-rise buildings during daily management and emergency response phases, thus promoting comprehensive pedestrian safety management and the development of smart fire safety and smart cities.

CRediT authorship contribution statement

Tong Lu: Writing – original draft, Validation, Methodology, Investigation. **Rong Deng:** Methodology, Investigation, Formal analysis. **Yuxin Zhang:** Writing – review & editing, Supervision, Funding acquisition. **Saizhe Ding:** Methodology, Investigation, Formal analysis. **Xinyan Huang:** Writing – review & editing, Supervision, Methodology, Funding acquisition, Conceptualization.

Declaration of competing interest

The authors declare that they have no known competing financial interests or personal relationships that could have appeared to influence the work reported in this paper.

Acknowledgements

This work is funded by the National Natural Science Foundation of China (52204232), and PolyU Start-up Fund under the Strategic Hiring Scheme (P0045772), and the Hong Kong Research Grants Council Theme-based Research Scheme (T22- 505/19-N).

Data availability

Data will be made available on request.

References

[1] M. Wang, H. Xu, The impact of building height on urban thermal environment in summer: a case study of Chinese megacities, PLoS One 16 (2021) e0247786, https://doi.org/10.1371/JOURNAL.PONE.0247786.
[2] M.L. Ivanov, W.K. Chow, Experimental and numerical evacuation study in tall office building, J. Build. Eng. 76 (2023) 107103, https://doi.org/10.1016/J.JOBE.2023.107103.
[3] K. Wang, G. Huang, H. Yu, H. Jiang, X. Gao, A novel data-driven triangular-type staircase layout design in personnel safety evacuation in high-rise buildings, J. Build. Eng. 84 (2024) 108429, https://doi.org/10.1016/J.JOBE.2023.108429.
[4] Y. Zhang, Y. Ding, X. Zhang, X. Huang, Multi-scale spatial-temporal principles of global evacuation safety based on pareto frontiers: a demonstration in tunnel, Tunn. Undergr. Space Technol. 166 (2025) 106950, https://doi.org/10.1016/j.tust.2025.106950.
[5] Y. Minegishi, Crowd management employing nudge theory for safe elevator use by masses of occupants during a high-rise building evacuation, J. Build. Eng. 111 (2025) 113529, https://doi.org/10.1016/J.JOBE.2025.113529.
[6] G. Proulx, Evacuation time and movement in apartment buildings, Fire Saf. J. 24 (1995) 229–246, https://doi.org/10.1016/0379-7112(95)00023-M.
[7] E.D. Kuligowski, Human Behavior in Fire, fifth ed., SFPE Handbook of Fire Protection Engineering, 2016, pp. 2070–2114, https://doi.org/10.1007/978-1-4939-2565-0_58.
[8] L. Sun, H. Liu, B. Fan, X. Li, W. Li, Multi-agent deep reinforcement Learning-based path planning for crowd evacuation in buildings, J. Build. Eng. 111 (2025) 113345, https://doi.org/10.1016/J.JOBE.2025.113345.

[9] R.D. Peacock, P.A. Reneke, E.D. Kuligowski, C.R. Hagwood, Movement on stairs during building evacuations, Fire Technol. 2 (53) (2016) 845–871, https://doi.org/10.1007/S10694-016-0603-5, 2016 53.

[10] M.L. Ivanov, W.K. Chow, Fire safety in modern indoor and built environment, Indoor Built Environ. 32 (2023) 3–8, https://doi.org/10.1177/1420326X221134765. Requestedjournal:Journal:Ibeb;Website:Website:Sage;Wgroup:String:Publication.

[11] M.L. Ivanov, W.K. Chow, T.K. Yue, H.L. Tsang, W. Peng, Upgrading of fire safety requirement for tall buildings in Bulgaria and proposal of implementing fire safety management under facility management, Facilities 40 (2022) 380–393, https://doi.org/10.1108/F-10-2021-0107.

[12] F. Wang, Y. Zhang, S. Ding, X. Huang, Optimizing phased-evacuation strategy for high-rise buildings in fire, J. Build. Eng. 95 (2024) 110084, https://doi.org/10.1016/J.JOBE.2024.110084.

[13] S.L. Poon, A dynamic approach to ASET/RSET assessment in performance based design, Procedia Eng. 71 (2014) 173–181, https://doi.org/10.1016/j.proeng.2014.04.025.

[14] H. Xu, Y. Wei, Y. Tan, Optimization of emergency evacuation in complex rail transit station, J. Build. Eng. 95 (2024) 110321, https://doi.org/10.1016/j.jobe.2024.110321.

[15] Y. Zhang, X. Zhang, X. Huang, Design a safe firefighting time (SFT) for major fire disaster emergency response, Int. J. Disaster Risk Reduct. 88 (2023) 103606, https://doi.org/10.1016/j.ijdrr.2023.103606.

[16] Buildings Department, Code of Practice for Fire Safety in Buildings 2011 (June 2023 Version), The Government of the Hong Kong Special Administrative Region, 2023.

[17] C. Chen, T. Lu, W. Jiao, C. Shi, An extended model for crowd evacuation considering crowding and stampede effects under the internal crushing, Phys. Stat. Mech. Appl. 625 (2023) 129002, https://doi.org/10.1016/J.PHYSA.2023.129002.

[18] N. Pelechano, A. Malkawi, Evacuation simulation models: challenges in modeling high rise building evacuation with cellular automata approaches, Autom. ConStruct. 17 (2008) 377–385, https://doi.org/10.1016/J.AUTCON.2007.06.005.

[19] C. Chen, T. Lu, An extended model for crowded evacuation considering stampede on inclined staircases, Simulat. Model. Pract. Theor. 135 (2024) 102978, https://doi.org/10.1016/j.simpat.2024.102978.

[20] J. Tan, W. Zhang, T. Nong, Z. Zhang, T. Wang, Y. Ma, E.W.M. Lee, M. Shi, An improved social force model based on nucleus force theory to simulate building evacuation in different visibility conditions, Simulat. Model. Pract. Theor. 142 (2025) 103117, https://doi.org/10.1016/J.SIMPAT.2025.103117.

[21] C. Li, F. Huo, T. Zhou, D. Wang, Y. Li, C. Jiang, Multifactor dynamic coupled model for building fire evacuation: case study of the karamay friendship palace fire, J. Build. Eng. 95 (2024) 110079, https://doi.org/10.1016/J.JOBE.2024.110079.

[22] Y. Zhang, W. Li, Y. Rui, S. Wang, H. Zhu, Z. Yan, A modified cellular automaton model of pedestrian evacuation in a tunnel fire, Tunn. Undergr. Space Technol. 130 (2022) 104673, https://doi.org/10.1016/J.TUST.2022.104673.

[23] BSI, BS 7974:2019, Application of Fire Safety Engineering Principles to the Design of Buildings, British Standards Institution, 2019.

[24] MOHURD, GB 50016-2014 Code for Fire Protection Design of Buildings, 2018 Edition, Ministry of Housing and Urban-Rural Development of the P.R.C., 2018.

[25] X. Liu, J. Huang, J. Zhao, Y. Ji, X. Fan, T. Du, Predicting temporal evacuation travel time in staircases between adjacent floors of super high-rise buildings by artificial neural networks, J. Build. Eng. 98 (2024) 111133, https://doi.org/10.1016/J.JOBE.2024.111133.

[26] X. Zhang, S. Dunn, Y. Luo, Y. Shen, Integrating human behaviors in an agent-based model for multi-floor building emergency evacuation, J. Build. Eng. 112 (2025) 113716, https://doi.org/10.1016/J.JOBE.2025.113716.

[27] A.R. Rasa, L. Xia, X. Song, H. Yu, R. Karim, J. Zhang, W. Song, Understanding human-obstacle interaction dynamics on staircases: implications for emergency evacuation and fire safety in high-rise buildings, J. Build. Eng. 98 (2024) 111082, https://doi.org/10.1016/j.jobe.2024.111082.

[28] Q. Wang, Y. Yu, L. Jin, Z. Zheng, J. Ding, L. Lu, Evacuation safety assessment in corridor-type high-rise building under fires, J. Build. Eng. 96 (2024) 110580, https://doi.org/10.1016/J.JOBE.2024.110580.

[29] Thunderhead Engineering, Pathfinder Technical Reference Manual, Manhattan, KS, USA, 2024.

[30] Y. Zeng, Z. Zheng, T. Zhang, X. Huang, X. Lu, AI-powered fire engineering design and smoke flow analysis for complex-shaped buildings, J Comput Des Eng 11 (2024) 359–373, https://doi.org/10.1093/jcde/qwae053.

[31] J. Han, Z. Zheng, Y. Gu, J.R. Lin, X.Z. Lu, Generative model-based building evacuation simulation for safety design, J. Build. Eng. 116 (2025) 114644, https://doi.org/10.1016/J.JOBE.2025.114644.

[32] T. Lu, Y. Zeng, Z. Zheng, Y. Zhang, X. Huang, X. Lu, AI-powered safe egress time assessment for complex building fire evacuation, J. Build. Eng. 110 (2025) 113013, https://doi.org/10.1016/j.jobe.2025.113013.

[33] T. Lu, Y. Zhang, W. Xie, X. Huang, Human-AI interactive framework for smart evacuation safety analysis in large infrastructures. Reliab Eng Syst Saf, 2025 111695, https://doi.org/10.1016/J.RESS.2025.111695.

[34] L. Zhang, A. Rao, M. Agrawala, Adding conditional control to text-to-image diffusion models, Proceedings of the IEEE International Conference on Computer Vision (2023) 3813–3824, https://doi.org/10.1109/ICCV51070.2023.00355.

[35] Y. Wu, C. Wu, L. He, S. Tong, Y. Song, M. Wang, Research on a ControlNet-based facade generation methodology for rural self-built houses with the goal of optimizing government-issued general-purpose design atlases, Front. Archit. Res. (2025), https://doi.org/10.1016/J.FOAR.2025.10.010.

[36] J. Li, W. Wang, B. Fu, Y. Gao, FrameDiffusion: a latent diffusion model for intelligent layout design of steel frame-braced structures, Eng. Struct. 343 (2025) 121195, https://doi.org/10.1016/J.ENGSTRUCT.2025.121195.

[37] S. Davari, D. Kim, A. Tohidifar, ControlNet-based domain adaptation for synthetic construction images via graphical simulation and generative AI, Autom. ConStruct. 180 (2025) 106562, https://doi.org/10.1016/j.autcon.2025.106562.

[38] H. Zheng, A diffusion-based machine learning method for 3D architectural form-finding, Front. Archit. Res. (2025), https://doi.org/10.1016/j.foar.2024.12.002.

[39] C. Chen, H. Sun, P. Lei, D. Zhao, C. Shi, An extended model for crowd evacuation considering pedestrian panic in artificial attack, Phys. Stat. Mech. Appl. 571 (2021) 125833, https://doi.org/10.1016/j.physa.2021.125833.

[40] W. Wu, Z. Zhu, X. Zheng, S. Liu, D. Zhang, Pedestrian vulnerability assessment of underground staircases in urban flooding, Sustain. Cities Soc. 131 (2025) 106700, https://doi.org/10.1016/j.scs.2025.106700.

[41] Y. Li, Q. Mao, Y. Li, M. Zuo, X. Wan, An evacuation model considering multi-attribute group decision-making behavior, Reliab. Eng. Syst. Saf. 268 (2026) 111976, https://doi.org/10.1016/J.RESS.2025.111976.

[42] Y. Ma, Z. Zhang, W. Zhang, E.W. Lee, M. Shi, Development of a time pressure-based model for the simulation of an evacuation in a fire emergency, J. Build. Eng. 87 (2024) 109069, https://doi.org/10.1016/J.JOBE.2024.109069.

[43] Y. Zeng, R. Ye, L. Lian, J. Sun, Exploring occupant evacuation characteristics in the stairwell through an evacuation drill and a microscopic model, Phys. Stat. Mech. Appl. 674 (2025) 130726, https://doi.org/10.1016/j.physa.2025.130726.

[44] F. Deng, J. Wang, D. Li, W. Lv, Z. Fang, Development of a three-stage hierarchical model for quick calculating stair evacuation time of high-rise building coupled with simulation analysis, Phys. Stat. Mech. Appl. 640 (2024) 129701, https://doi.org/10.1016/J.PHYSA.2024.129701.

[45] Y. Zhang, Y. Ding, M. Chraibi, X. Huang, Multi-scale analysis of fire and evacuation drill in a multi-functional university high-rise building, developments in the, Built. Environ. 21 (2025) 100626, https://doi.org/10.1016/J.DIBE.2025.100626.

[46] T. Sano, E. Ronchi, Y. Minegishi, D. Nilsson, Modelling pedestrian merging in stair evacuation in multi-purpose buildings, Simulat. Model. Pract. Theor. 85 (2018) 80–94, https://doi.org/10.1016/j.simpat.2018.04.003.